

## Supporting Information

# Multifunctional stimuli-responsive cellulose nanocrystals *via* dual surface modification with genetically engineered elastin-like polypeptides and poly(acrylic acid)

Jani-Markus Malho<sup>\*, α, †</sup>, Jérémie Brand<sup>α</sup>, Gilles Pecastaings<sup>α</sup>, Janne Ruokolainen<sup>β</sup>, André Gröschel<sup>γ</sup>, Gilles Sèbe<sup>α</sup>, Elisabeth Garanger<sup>\*, α</sup>, Sébastien Lecommandoux<sup>α</sup>

<sup>α</sup> Laboratoire de Chimie des Polymères Organiques (LCPO), CNRS UMR5629, Université de Bordeaux, Bordeaux-INP, Pessac 33607 Cedex, France

<sup>β</sup> Department of Applied Physics, Aalto University School of Science, P.O. Box 15100, 00076 Aalto, Finland

<sup>γ</sup> Physical Chemistry and Center for Nanointegration (CENIDE), University of Duisburg-Essen, 45127 Essen, Germany

### Corresponding Authors

\* E-mail: [janimarkus.malho@gmail.com](mailto:janimarkus.malho@gmail.com)

\* E-mail: [garanger@enscbp.fr](mailto:garanger@enscbp.fr)

### Contents

|  |           |
|--|-----------|
| <b>MATERIALS AND METHODS</b>   | <b>2</b>  |
| ZETA POTENTIAL MEASUREMENTS  | 2         |
| ULTRAVIOLET-VISIBLE SPECTROSCOPY (UV-VIS)                                | 2         |
| SIZE EXCLUSION CHROMATOGRAPHY (SEC)                                      | 2         |
| ELEMENTAL ANALYSIS (EA)  | 2         |
| FOURIER TRANSFORM INFRARED SPECTROSCOPY (FT-IR)                          | 2         |
| THERMO-GRAVIMETRIC ANALYSIS (TGA)  | 3         |
| CRYO-TRANSMISSION ELECTRON MICROSCOPY (CRYO-TEM)                         | 3         |
| ATOMIC FORCE MICROSCOPY (AFM)  | 3         |
| LIGHT MICROSCOPY   | 3         |
| <b>EXPERIMENTAL SECTION</b>  | <b>4</b>  |
| SURFACE ESTERIFICATION OF SOXHLET-EXTRACTED CNCs VIA BIBB                | 4         |
| SURFACE MODIFICATION OF CNCs WITH PMPI                                   | 4         |
| QUANTIFICATION OF PMPI AND BIBB BASED ON THE EA                          | 5         |
| ELP CONJUGATION OF THE DUAL-MODIFIED CNCs                                | 6         |
| SURFACE INITIATED ATOM TRANSFER RADICAL POLYMERIZATION (SI-ATRP) OF CNCs | 6         |
| LENGTH OF THE PtBA   | 7         |
| FT-IR MEASUREMENTS   | 8         |
| UV-VIS QUANTIFICATION  | 11        |
| <b>SUPPORTING REFERENCES</b>   | <b>13</b> |

## Materials and Methods

The cellulose nanocrystals (CNCs) were provided by the university of Maine (USA) ( $D = 6$  nm,  $L = 110$  nm, with 1.05 wt. % of sodium sulfate). Therein, the CNCs were extracted by acidic hydrolysis with sulfuric acid from softwood, neutralized with NaOH and freeze dried to afford a dry powder.  $\alpha$ -bromoisobutyryl bromide (97 %) (BIBB) was purchased from Alfa Aesar and ethyl  $\alpha$ -bromoisobutyrate (EBIB) (98 %) from Sigma Aldrich. Pentamethyldiethylenetriamine (99 %) (PMDETA) was purchased from Sigma Aldrich. *P*-maleidophenyl isocyanate (PMPI) was purchased from Fisher Scientific and was directly transferred to a glove box to avoid moisture and oxygen. Each bottle of PMPI (50 mg) was mixed with 1 mL of anhydrous DMF prior to the reaction. Elastin like polypeptides (ELPs) were produced in *Escherichia coli* bacteria according to a previously described procedure (Bataille, L. *et al. Protein Expr. Purif.* **2016**, *121*, 81–87). The primary sequence of the ELP used in the study is MW(VPGIG)<sub>20</sub>C. The peptide contains one tryptophan (W) for quantification by UV-Vis and one cysteine residue (C) for reaction with the PMPI-modified CNCs. *Tert*-butyl acrylate (99 %) (*t*BA) was purchased from Alfa Aesar.

### Zeta potential measurements

Measurements were carried out on a Malvern ZetaSizer (ZS90) equipment. Samples were dispersed in water in a polycarbonate cell at 0.5 mg/mL. The sample and the cell were cooled down in cold water and the measurement started immediately after. The measurement temperature was set at 25 °C and the sample was allowed to warm up in the cell. The zeta potential was followed over a time frame of 30 minutes from the cold state to 25 °C to check if the zeta potential was changing due to the ELPs, which aggregate beyond their transition temperature.

### Ultraviolet-visible spectroscopy (UV-vis)

UV-Vis spectroscopy was carried out on a thermostated Agilent Carry 4000 spectrometer. For all samples, the pH was adjusted to 8.5 and the concentration to 0.5 g/L in Quartz cells. The dispersions were analyzed at 10 °C and at 35 °C. The scanning region was set from 200 to 500 nm with a scanning speed of 600 nm/min. The Spectral Band Width (SBW) was 4 nm.

### Size exclusion chromatography (SEC)

SEC analysis was carried out on a Malvern GPC2155 instrument. The samples were prepared in chloroform at 3 g/L with TCB (0.15 wt %) as flow marker. The temperature was set to 30 °C and the flow rate was set to 1 mL/min.

### Elemental analysis (EA)

C, H and N elemental analysis were obtained by thermal conductivity (MO 240 LA2008 (COFRAC), ASTM D 5291 (COFRAC)), O and S elemental analysis were obtained by infrared analysis (MO 238 LA 2008 (COFRAC)). All analysis were performed by SGS Multilab (Evry, France).

### Fourier transform infrared spectroscopy (FT-IR)

Infrared spectra of CNCs were recorded using a Thermo Nicolet FT-IR spectrometer (AVATAR 370) in transmission mode. For each analysis, 2 mg of sample were mixed with 180 mg of KBr. All spectra were recorded from 400 to 4000  $\text{cm}^{-1}$  with an 8  $\text{cm}^{-1}$  resolution and 64 scans. To compare samples, the same baseline correction was used and the spectra were normalized to the C-O stretching vibration of glucopyranose ring at 1060  $\text{cm}^{-1}$ , which is not affected by the chemical modification.

### **Thermo-gravimetric analysis (TGA)**

Thermo-gravimetric analyses (TGA) were performed on a TA Q500 instrument to characterize the CNC before and after modifications. Samples were heated from room temperature to 60 °C at a rate of 15 °C/min under a nitrogen flow, held at 60 °C for 20 minutes and then heated to 600 °C at the same speed. This plateau was applied to further dry the samples inside the TGA. The weight measured at the end of this plateau was considered as the initial sample weight.

### **Cryo-transmission electron microscopy (Cryo-TEM)**

Cryo-transmission electron microscopy (Cryo-TEM) imaging was carried out using Jeol's 3200FSC cryo-transmission electron microscope, which was operated at 300 kV in bright field mode. The imaging was performed with an Omega-type Zero-loss energy filter and the images were acquired with Gatan Ultrascan 4000 CCD camera. The specimen temperature was maintained at -187 °C throughout the imaging. Vitrified samples were prepared using a Fei Vitrobot by pipetting 3 µL of sample dispersion on to holey carbon copper grids under 80-100% humidity. The blotting chamber temperature was varied due to the temperature sensitive nature of the ELPs, which had a transition temperature of approximately +20°C. Hence, the first sample was cooled down to approximately of 10°C prior the blotting for one of the samples, while the vitrobot chamber was maintained at +23°C during the sample preparation of the second sample. The samples were blotted with a filter paper for 1.5–2.5 seconds followed by an immediate plunging into -170°C ethane/propane mixture. The samples were then cryo-transferred into the cryo- transmission electron microscope for imaging.

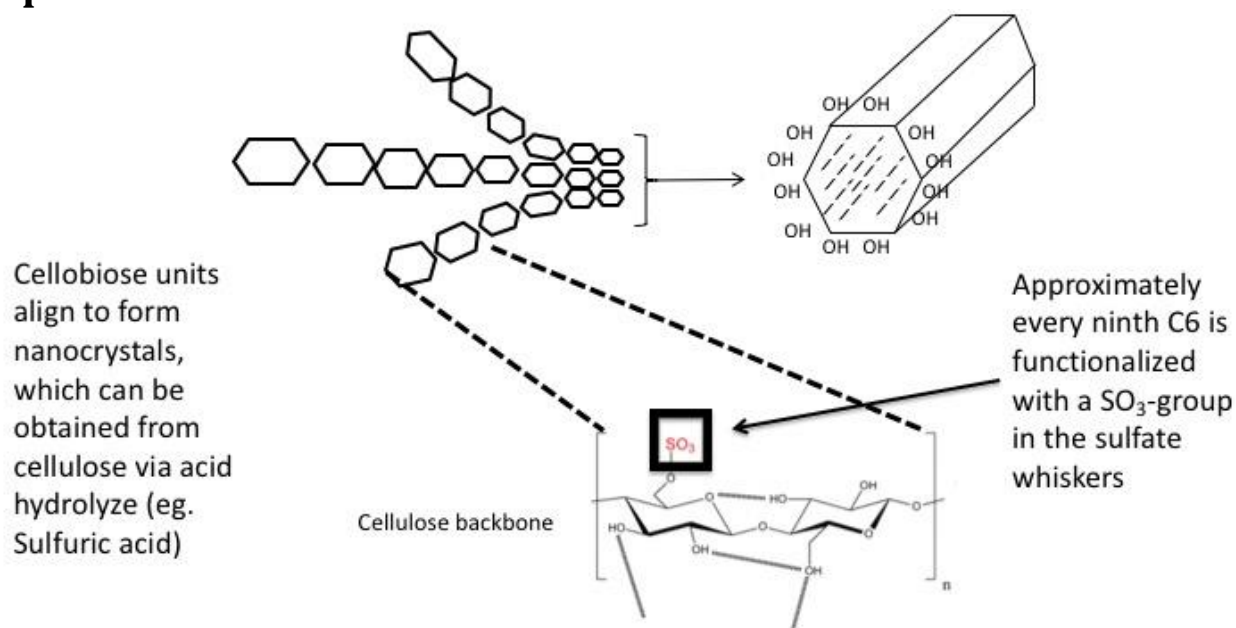
### **Atomic force microscopy (AFM)**

Atomic force microscopy was performed in tapping mode at 22 °C using a Dimension FastScan Bruker AFM system. Silicon cantilevers (FastScan-A) had a typical tip radius of 5 nm, a cantilever resonance was set to 1400 kHz and a spring constant of 18 N/m was used. Samples were prepared by drop-casting a CNCs suspension of 0.005 mg/mL onto a freshly cleaved mica surface, which was subsequently let to dry overnight at room temperature.

### **Light microscopy**

Optical microscopy was performed with Zeiss AX-10 microscope, which was equipped with a thermally controllable plate. Polarized light was used to increase the contrast.

## Experimental Section



Amount OH-groups on the CNC surface is approx 2.0 mmol/g and the amount of  $\text{SO}_3$  on the CNC surface is approx 0.3 mmol/g.

**Scheme S1. Schematic representation of cellulose nanocrystals with respect to the cellobiose units and the surface hydroxyls.**<sup>1,2</sup>

### Surface esterification of soxhlet-extracted CNCs via BIBB

Sulfuric acid hydrolyzed cellulose nanocrystals were first purified by ethanol via soxhlet extraction method<sup>1</sup> and subsequently freeze-dried to form an aerogel. To facilitate the SI-ATRP, the cellulose nanocrystals were functionalized via chemical vapor deposition (CVD), wherein approximately 1 mL of  $\alpha$ -bromoisobutyryl bromide (BIBB) was closed in a desiccator with 1,000 mg of CNCs overnight. The CNCs and BIBB were kept in separate containers inside the desiccator. The excess amount of BIBB was removed from the CNCs via washing twice with dichloromethane (DCM) and twice with acetone. The CNC dispersions were centrifuged (8000 rpm, 10 min) between every washing step and the supernatants were removed. At the end, the brominated CNCs were dried from acetone via rotavap for further modification. The amount of bromination was confirmed by Fourier transform infrared spectroscopy (FT-IR) and elemental analysis (EA). The results revealed approximately 10% degree of substitution in relation to the free surface hydroxyls on CNCs, which is comparable to the previously reported values.<sup>3,4</sup>

### Surface modification of CNCs with PMPI

150 mg of dried and brominated cellulose whiskers were weighted in to a flask after under vacuum for two hours to remove any remaining moisture. Removal of water is critical as the CNCs, even when brominated, are amphiphilic by nature and any remaining water will reduce the yield of PMPI modification. We utilized here approximately an equimolar amount of PMPI in relation to the calculated amount of free OH-groups on cellulose nanocrystals surface, which is approximately 2.0 mmol/g for unmodified cellulose nanocrystals. In the case of sulfate whiskers part of the OH-groups are occupied by sulfate groups and herein also by the BIBB, lowering the amount of free surface hydroxyls for the PMPI modification, because the sulfate and BIBB modified hydroxyls do not react with the PMPI. We calculated the amount of sulfate groups to be approximately 0.3 mmol/g based on elemental analysis and the

information provided by the supplier (University of Maine, USA). Thus, we utilized here excess amount of PMPI in relation to free OH-groups, in addition all of the surface hydroxyls (particularly the C3 hydroxyl) are not easily modified.<sup>1</sup> 9mL of dry-DMF was added to the 150 mg of brominated CNCs under nitrogen and magnetic stirring was applied to disperse the brominated CNCs. 50 mg of PMPI was dissolved in 1mL of dry-DMF in glove box and injected to the CNC-BIBB dispersion inside the glove box to avoid any oxygen and humidity in the reaction. The reaction mixture was stirred overnight at room temperature under nitrogen and an aluminum foil was used to protect the sample from light. The reaction was stopped by addition of methanol (100  $\mu$ l), after which the sample was washed two times with tetrahydrofuran (THF) and once with acetone to remove the excess amount of unattached PMPI. The sample was centrifuged (8000 rpm, 10 minutes) between every washing cycle and the supernatant removed. Finally, the CNC-BIBB-PMPI was dispersed in DMF for further modification. The PMPI modification was confirmed by FT-IR and NMR, and quantified by EA.

### Quantification of PMPI and BIBB based on the EA

**Table S1. Elemental analysis of the PMPI modified CNCs**

| Element | Content (wt. %) |          |          |
|---------|-----------------|----------|----------|
|         | CNC             | CNC-PMPI | CNC-BIBB |
| C       | 42.0            | 41.7     | -        |
| H       | 6.1             | 6.09     | -        |
| N*      | -               | 0.14     | -        |
| O       | 51.08           | 50.5     | -        |
| S       | 1.04            | 0.8      | -        |
| Br      | -               | -        | 1.65     |

\*Unmodified CNCs have less than 0.05% of nitrogen, which is below the detection limit.

The grafting level on CNC surface has been estimated after reaction with PMPI or BIBB. These grafting densities are considered as the highest modification level we can reach for each function on soxhlet extracted CNCs. These calculations were conducted based on EA results: nitrogen content has been used to estimate the PMPI grafting level (CNC-PMPI) and the Bromide content for BIBB (CNC-BIBB). For BIBB content, the value is an average of three measurements. Then, the fraction of modified OH groups on CNC surface can be calculated. We assume here that unmodified CNC have approximately 2,17 mmol of OH groups per gram of CNC, based on our calculation and in accordance with values found by chemical derivatization in literature<sup>5</sup>.

Estimation of the PMPI grafting level:

We used the elemental analysis results to estimate the PMPI reactivity with surface hydroxyls of the CNCs. Based on Brand *et al.* the amount of free surface hydroxyls is 2.17 mmol/g of CNC, which was measured by NMR<sup>5</sup>. The amount of nitrogen was found to be 0.14 wt% on the CNCs, which equals to 0.05 mmol of PMPI ( $M_w = 214,18$  g/mol). From this we get a fraction of 2.5% of PMPI attached to the free surface hydroxyls of CNC which is approximately 2.5  $\mu$ mol.

Estimation of Br grafting level:

We used the elemental analysis results to estimate the BIBB reactivity with surface hydroxyls of the CNCs. Based on Brand *et al.* the amount of free surface hydroxyls is 2.17 mmol/g of CNC, which was measured by NMR<sup>5</sup>. We found an average of 1.65 wt% of bromide in CNC-BIBB. Bromide has a molecular weight of 79 g/mol, which gives 0.2 mmol of bromide per gram of CNC, which suggests that approximately 10% of the total amount of the free surface hydroxyl groups on CNC are brominated.

### **ELP conjugation of the dual-modified CNCs**

Next, we conjugated the ELPs with CNCs through the attached PMPIs. Every single ELP chain has one cysteine residue with one thiol-function; herein we used ELPs with two-fold excess molar ratio in relation to the amount of attached PMPIs on CNC surface. Some of the ELPs are most likely dimerized via disulfide-bridges, making them inert to the reaction and thus reducing the yield of ELP grafting. Approximately 100 mg of dried ELPs were added to a 4.5 mL of the CNC-BIBB-PMPI in DMF, in which the amount of CNC-BIBB-PMPI was 10 mg/mL. The reaction mixture was stirred overnight at room temperature and protected from light via aluminum foil. The sample was washed twice with THF, once with acetone and eventually dispersed in small amount of water prior to freeze-drying. The sample was centrifuged (9000 rpm, 10 minutes) between every washing cycle and the supernatant was removed. The washing was carried out to remove the DMF prior the drying. The attachment of the ELPs was qualitatively confirmed by cryo-transmission electron microscopy (cryo-TEM) and atomic force microscopy (AFM). The cryo-TEM sample preparation was carried out both below and above the transition temperature (approx. 20°C) of these ELPs<sup>6</sup> to visualize the collapse and aggregation of the CNC-ELP hybrids.

### **Surface initiated atom transfer radical polymerization (SI-ATRP) of CNCs**

The SI-ATRP was carried out following previously reported protocol.<sup>4</sup> Herein, the esterification was performed in one step using only CVD to control the density of the brominated hydroxyl groups to enable the addition of rigid PMPI molecules, which was carried out after the bromination. This was done due to possible steric hindrance that is likely to occur with dense bromination on the CNC surfaces, furthermore the polymerization was performed after the attachment of ELPs, because the monomer is expected to diffuse more easily to the ELP grafted CNC surface than the relatively large ELPs. We carried out SI-ATRP on CNC-BIBB in the absence of PMPI as a reference sample. ATRP was performed for both CNC-BIBB-PMPI-ELP and CNC-BIBB in the presence of 10 µl of ethyl  $\alpha$ -bromoisobutyrate (EBiB) as a sacrificial initiator to determinate the length of the polymer chains. Sacrificial initiator is generally accepted as a good reference to determine the length of the brushes on the CNC surface.

150 mg of CNC-BIBB-PMPI-ELPs were measured to a flask. A vacuum was applied for approximately one hour to remove oxygen, which can hinder the catalyst, Cu(I)Br. Next, the CNC-BIBB-ELPs were dissolved in 3 mL of dry DMF, after which 5 mL of *tert* butyl acrylate (*t*BA) monomer, 20 µl of pentamethyldiethylenetriamine (PMDETA) and 10 µl EBiB were added to the mixture. The mixture was stirred with magnetic stirrer and bubbled with nitrogen (N<sub>2</sub>) for approximately 30 minutes before the addition of 10 mg of the catalyst Cu(I)Br, which was done in a glove box to avoid oxygen in the reaction. The mixture subsequently was set to an oil bath and stirred overnight at +70°C, using aluminum foil to protect the sample from light. The reaction was stopped by addition of excess amount of methanol to the mixture. The sample CNC-ELP-PtBA was washed twice with methanol, twice with water, twice with acetone, dispersed in to water and freeze-dried. The sample was centrifuged (8000 rpm, 10 min) between every washing cycle and the supernatant was

removed. To generate anionic polymer brushes the poly(*tert* butyl acrylate) (PtBA) chains were hydrolyzed with trifluoroacetic acid (TFA) to yield CNC-ELP-PAA brushes. The CNC-ELP-PAA and CNC-PAA samples were visualized via cryo-TEM and AFM; the CNC-PAA samples have been visualized before *via* cryo-TEM.<sup>3</sup>

### Length of the PtBA

The PtBA grafting level has been estimated by combining several experimental results. The polymer degradation has been observed in two steps at 216 and 443 °C under nitrogen atmosphere by TGA. Mass losses are 70 and 30 wt.%, respectively.

In the case of CNC-ELP-PtBA and CNC-PtBA, the first PtBA peak at 216 °C was easy to integrate due to an isolated peak from other peaks in the TGA spectrum. Next, we were able to estimate the PtBA content by integrating the first peak and adding 30 % to get the complete polymer mass. Based on the 216 °C peak integration, we estimated the PtBA amount to be 6 and 7 wt.% for CNC-PtBA and CNC-ELP-PtBA, respectively, suggesting that the polymerization has not been affected much by the grafted or the free ELPs. The total weight of the grafted PtBA would be changed, because the CNC-PtBA and CNC-ELP-PtBA were washed from the excess of ELPs, the free homopolymer, monomer and other impurities after the ATRP reaction, leaving only the grafted supramolecular CNC complexes in the measured samples.

To determine the PtBA surface grafting level, we used the SEC measured molecular weight of the free polymer in the reaction medium. We assume, based on previous ATRP work from the literature, that the polymer chain length is close to equivalent between the CNCs surface and the free chains in the solvent, which is generally accepted as a good principle. The grafted initiator and the sacrificial initiator in the medium were identical, which is a mandatory for this calculation. Based on the above-mentioned assumption and measurements, the PtBA content can be calculated in moles per gram for the grafted CNCs. For the CNC-ELP-PtBA we found 7 wt.% of PtBA. The polymer molecular weight is around  $M_n = 30\ 000$  g/mol based on the SEC. Hence, the number of moles are:

$$n(\text{PtBA}) = 0.07/30000 = 2.33 \mu\text{mol per gram of PtBA in CNC-ELP-PtBA}$$

With 30 wt.% of ELP in the same sample based on the UV-vis measurement and subsequent calculations,

$$n(\text{CNC}) = (100 \cdot 2.33)/0.63 = 3.70 \mu\text{mol per gram of CNC}$$

The PtBA length with 30 000 g/mol can be calculated based on the theoretical PtBA unit length with the C-C bonding length:

The molecular weight of a *t*BA unit is  $M = 128$  g/mol. Based on the SEC, the number of *t*BA unit per polymer chain is  $30000/128 = 234$ . In one unit, we have 3 times the C-C bond length. One C-C bond represents 0.154 nm. The angle formed between 3 successive carbons in one linear chain is 109.5 °. Moreover, we have 0.244 nm between the first and the third carbon. In theory, the *t*BA unit is  $0.244 + 0.122 = 0.366$  nm long. One PtBA chain would be  $234 \cdot 0.366 = 86$  nm in the fully stretched state, which was used to compare with the measured width from the AFM images, in which the samples are dried and thus not entirely comparable to solvated polymer chains.

## FT-IR measurements

Table S2. FT-IR bands for unmodified CNCs.

| Vibration type  | Wavenumbers (cm <sup>-1</sup> ) |            |
|---|---------------------------------|------------|
|   | Literature                      | Assignment |
| $\nu$ OH (hydrogen bonded)  | 3352                            | 1          |
| $\nu$ CH  | 2901                            | 2          |
| H <sub>2</sub> O  | 1640                            | 3          |
| $\delta$ CH <sub>2</sub> (sym) at C <sub>6</sub>  | 1431                            | 4          |
| $\delta$ CH   | 1373                            | 5          |
| $\delta$ CH(sym)  | 1331                            | 6          |
| $\delta$ CH <sub>2</sub> (wagg) at C <sub>6</sub>   | 1319                            | 7          |
| $\delta$ CH   | 1282                            | 8          |
| $\delta$ COH in plane at C <sub>6</sub>   | 1236                            | 9          |
| $\delta$ COH in plane at C <sub>6</sub>   | 1202                            | 10         |
| $\nu$ COC $\beta$ linked  | 1165                            | 11         |
| $\nu$ C-O at C <sub>2</sub>   | 1111                            | 12         |
| $\nu$ C-O at C <sub>3</sub>   | 1060                            | 13         |
| $\nu$ CO at C <sub>6</sub>  | 1032                            | 14         |
| $\nu$ CO at C <sub>6</sub>  | 983                             | 15         |
| $\nu$ COC liason $\beta$ ; $\nu$ COC, $\nu$ CCO, $\nu$ CCH at C <sub>5</sub> & C <sub>6</sub> | 897                             | 16         |
| $\delta$ (C-H)  | 806                             | 17         |
| $\delta$ (C-OH) out of plane  | 702                             | 18         |
| $\delta$ (C-OH) out of plane  | 665                             | 19         |
| $\nu$ OH  | 606                             | 20         |
| $\nu$ OH  | 550                             | 21         |

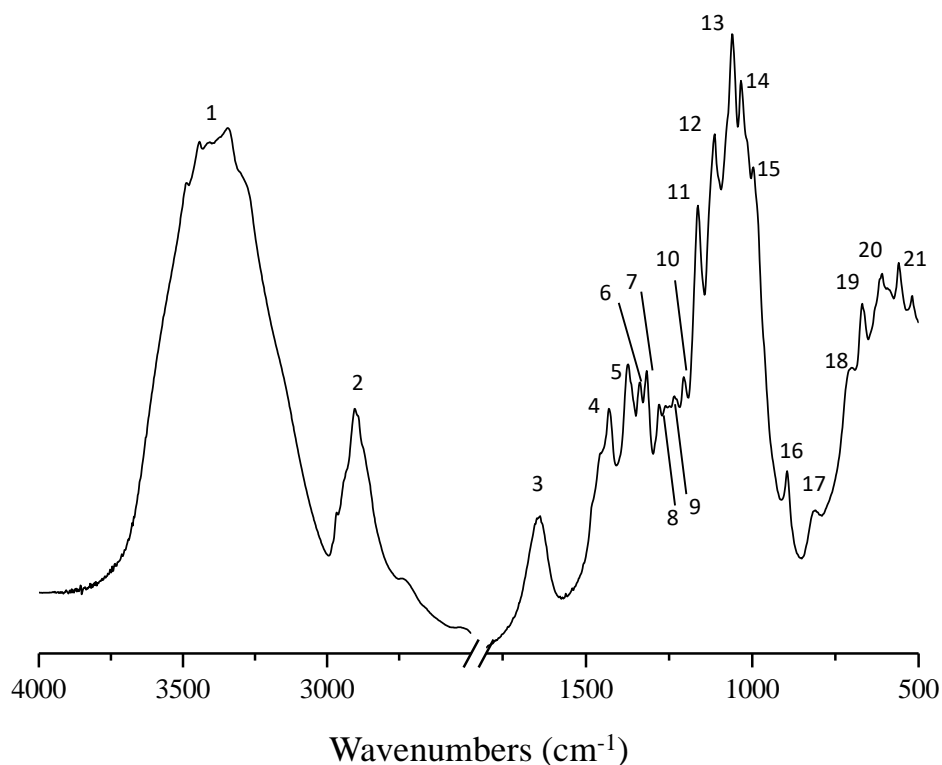


**Figure S1.** FT-IR spectrum of an unmodified cellulose nanocrystal.

**Table S3.** FT-IR bands for ATRP initiated CNC-BIBB and for ATRP polymerized CNC-PtBA, CNC-PAA and CNC-ELP-PAA.

| Vibration type         | Wavenumber (cm <sup>-1</sup> ) |
|------------------------|--------------------------------|
| v(C=O) TFA             | 1788                           |
| v(C=O) BIBB (shoulder) | 1730                           |
| v(C=O) PtBA            | 1732                           |
| v(C=O) PAA (shoulder)  | 1680                           |

**Table S4.** FT-IR band for CNC-PMPI.

| Vibration type                      | Wavenumbers (cm <sup>-1</sup> ) |
|-------------------------------------|---------------------------------|
| v (C=O)                             | 2270                            |
| v(C=O) sym. maleimide               | 1774                            |
| v(C=O) urethane                     | 1717                            |
| v(C=O) asvm. maleimide <sup>7</sup> |                                 |
| v(C=C) aromatic                     | 1640                            |
| H <sub>2</sub> O                    | 1640                            |

|                             |      |
|-----------------------------|------|
| $\delta(\text{N-H})$        | 1543 |
| $\nu(\text{=C-H})$ aromatic | 1511 |
| $\nu(\text{C-N-C})^8$       | 1400 |

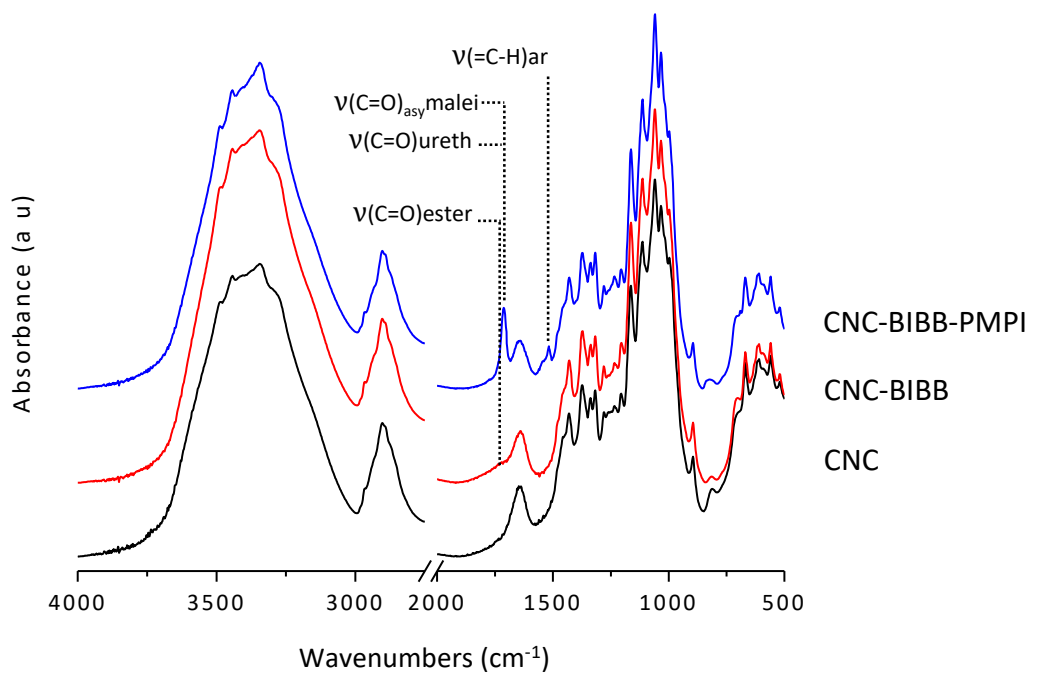


**Figure S2.** FT-IR spectra of unmodified CNC (black curve), CNC with BIBB modification (red curve) and CNC with dual modification with BIBB and PMPI (blue curve).

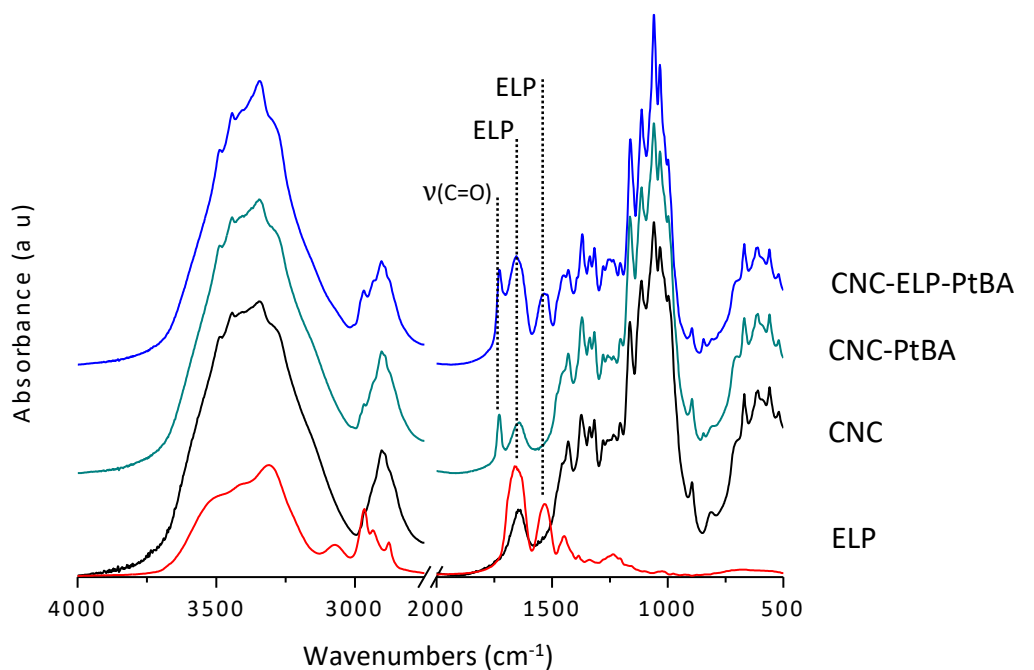


Figure S3. FT-IR spectra of unmodified CNC, ELP, CNC-PtBA and CNC-ELP-PtBA.

#### UV-vis quantification

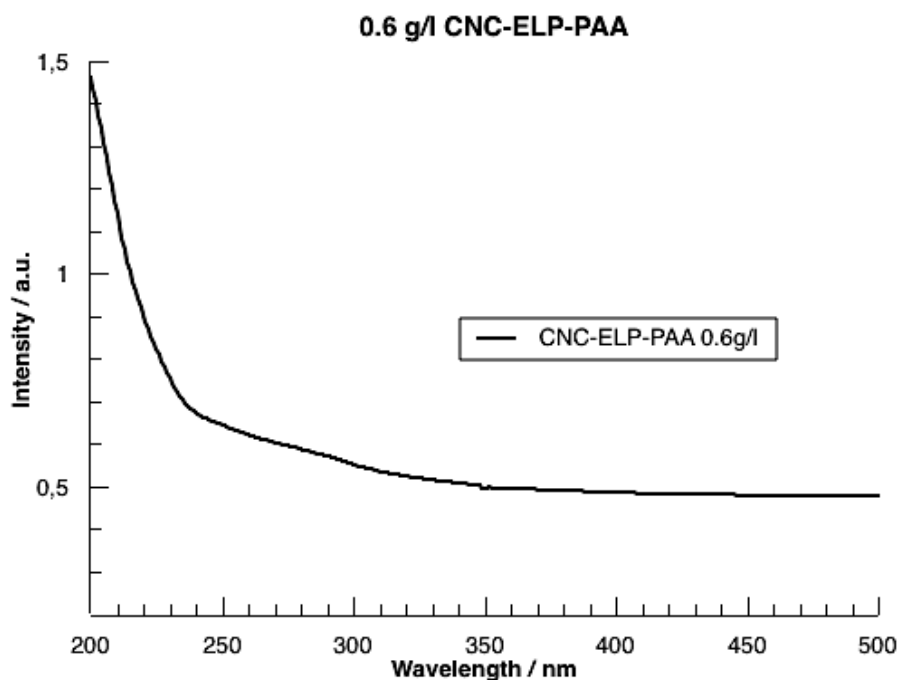


Figure S4. UV-vis spectroscopy on the CNC-ELP-PAA. CNC-ELP-PAA was weighted on a glass tube and diluted to 0.6 g/L for the UV-vis measurement. The pH was adjusted to 8.4.

UV-Vis quantification of the ELPs on CNC-ELP-PAA:

Molecular weight: 8908.81

Ext. coefficient ( $\epsilon$ ): 5500

Abs 0.1% (=1 g/l) 0.617, assuming all Cys residues are reduced

Intensity values at 280nm for CNC-ELP-PAA (0.6 g/l) = 0.586927176

Intensity values at 450nm for CNC-ELP-PAA (0.6 g/l) = 0.479061067

Normalized UV-vis value (280nm – 450nm) for CNC-ELP-PAA (0.6 g/l) = 0.107866109

Peptide concentration was calculated in mg/ml using the following equation,

$$C_{\text{ELP}} = (A_{280} \times M_w) / \epsilon,$$

Wherein the  $C_{\text{pep}}$  is the calculated concentration of the peptide,  $A_{280}$  is the normalized intensity value of the sample at 280 nm,  $M_w$  is the molecular weight and the  $\epsilon$  is the extinction coefficient of the ELP peptide.

$C_{\text{ELP}}$  is 0.175 g/l, which is 29% of the total mass of the CNC-ELP-PAA sample (0.6 g/l).

**Table S5. SEC results from CNC-PtBA and CNC-ELP-PtBA.**

|                        | CNC-PtBA | CNC-ELP-PtBA |
|------------------------|----------|--------------|
| <b>Mn (Chloroform)</b> | 31 000   | 29 000       |
| <b>PDI</b>             | 1.2      | 1.3          |

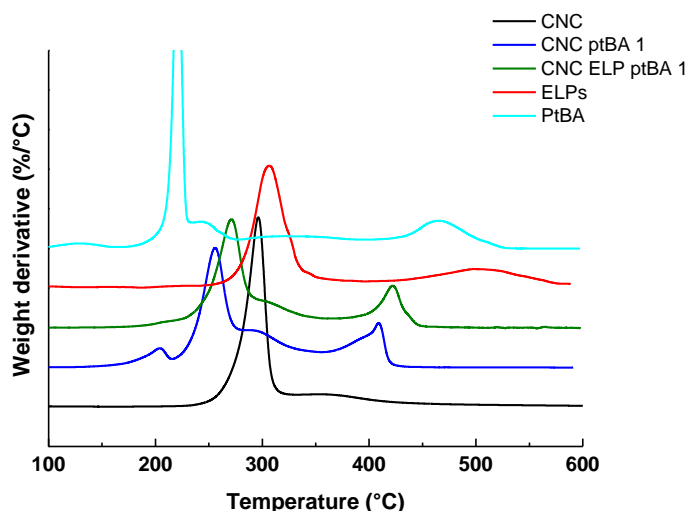


**Figure S5. Thermogravimetry profile of 7 wt.% of PtBA in CNC-ELP-PtBA, 6 wt.% of PtBA in CNC-PtBA only 60% of PtBA homopolymer degrades at around 200 °C.**

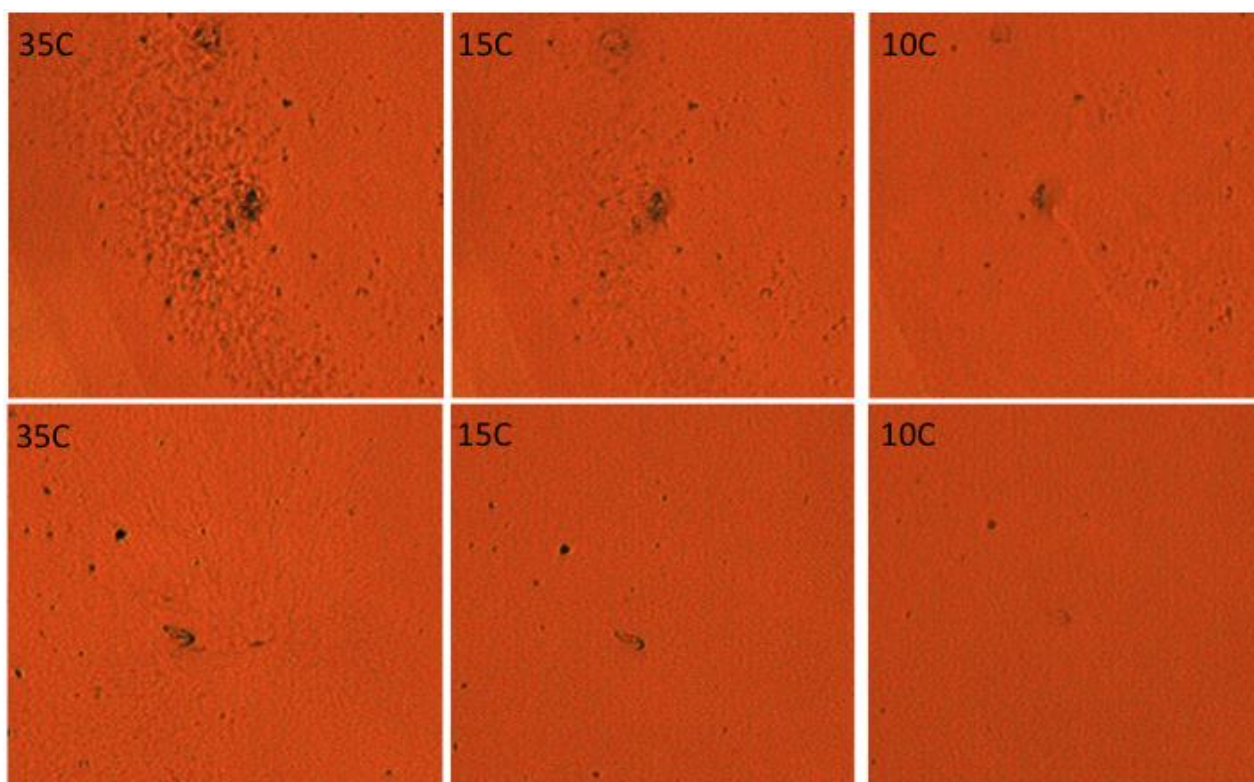


**Figure S6. Light microscopy images of CNC-ELP-PAA dispersion with a 0.5 g/L of solid content. The still images are taken at the same focal level at different temperatures. The images exhibit macroscopic reversible flocculation above LCTS and more homogenous dispersion of the CNC-ELP-PAA. Yet, some aggregates remain visual suggesting an ideal colloidal stability of the double brush decorated CNCs.**

## Supporting References

- (1) Eyley, S. S.; Thielemans, W. Surface modification of cellulose nanocrystals. *Nanoscale* **2014**, *6* (14), 7764–7779.
- (2) Habibi, Y.; Lucia, L. A.; Rojas, O. J. Cellulose Nanocrystals: Chemistry, Self-Assembly, and Applications. *Chem. Rev.* **2010**, *110* (6), 3479–3500.
- (3) Malho, J.-M.; Morits, M.; Löbbling, T. I.; Nonappa; Majoinen, J.; Schacher, F. H.; Ikkala, O.; Gröschel, A. H. Rod-Like Nanoparticles with Striped and Helical Topography. *ACS Macro Lett.* **2016**, *5* (10), 1185–1190.
- (4) Majoinen, J.; Walther, A.; McKee, J. R.; Kontturi, E.; Aseyev, V.; Malho, J. M.; Ruokolainen, J.; Ikkala, O. Polyelectrolyte Brushes Grafted from Cellulose Nanocrystals Using Cu-Mediated Surface-Initiated Controlled Radical Polymerization. *Biomacromolecules* **2011**, *12* (8), 2997–3006.
- (5) Brand, J.; Pecastaings, G.; Sèbe, G. A Versatile Method for the Surface Tailoring of Cellulose Nanocrystal Building Blocks by Acylation with Functional Vinyl Esters. *Carbohydr. Polym.* **2017**, *169*, 189–197.
- (6) Bataille, L.; Dieryck, W.; Hocquellet, A.; Cabanne, C.; Bathany, K.; Lecommandoux, S.; Garbay, B.; Garanger, E. Elastin-like Polypeptides with Low Transition Temperatures. *Protein Expr. Purif.* **2016**, *121*, 81–87.
- (7) Shen, G.; Anand, M. F. G.; Levicky, R. X-ray photoelectron spectroscopy and infrared spectroscopy study of maleimide-activated supports for immobilization of oligodeoxyribonucleotides *Nucleic Acids Res.* **2004**, *32* (20), 5973–5980.

- (8) Thielemans, W.; Belgacem, M. N.; Dufresne, A. Starch nanocrystals with large chain surface modification. *Langmuir* **2006**, *22* (10), 4804–4810.